Supplementary Information

1 Numerical calculation of mixing parameter

To compare with our experimental definition of mixing parameter Λ_M (equations 18-20 in the main text), we require a numerical definition to post-process our calculation.

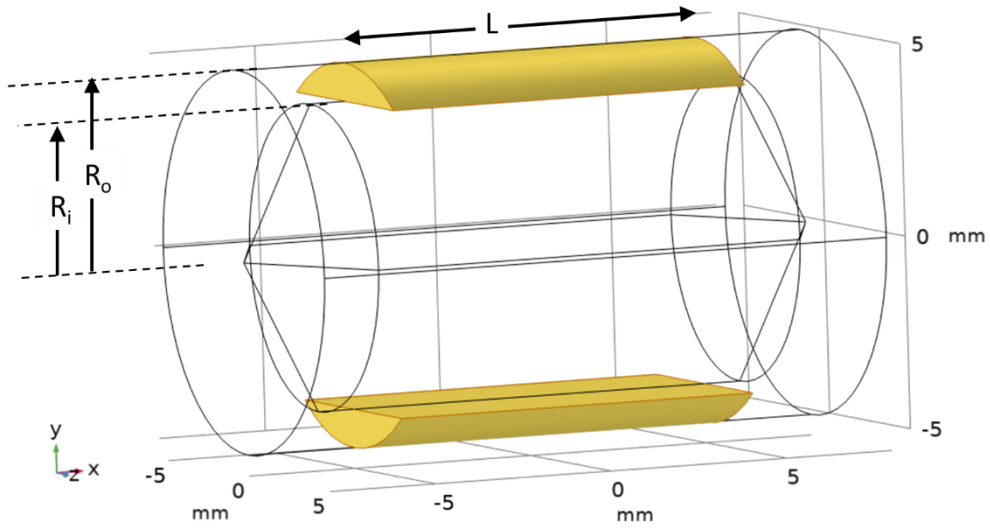

Figure S 1 Schematic of the geometry and parameters used for the definition of the lift parameter. Integration domains shaded in yellow.

This parameter can be calculated numerically using the following expression:

$$\Lambda = \frac{2\int_{R_i}^{R_o}\int_{-\frac{L}{2}}^{\frac{L}{2}}\int_{\sqrt{R_i^2-y^2}}^{\sqrt{R_o^2-y^2}} \phi.dx.dy.dz}{\int_{-R_o}^{-R_i}\int_{-\frac{L}{2}}^{\frac{L}{2}}\int_{\sqrt{R_i^2-y^2}}^{\sqrt{R_o^2-y^2}} \phi.dx.dy.dz + \int_{R_i}^{R_o}\int_{-\frac{L}{2}}^{\frac{L}{2}}\int_{\sqrt{R_i^2-y^2}}^{\sqrt{R_o^2-y^2}} \phi.dx.dy.dz} \quad (1)$$

where, L is the length of shaded domains in Figure S 1.

Using Λ *(numerical)*, the integral of the solid concentration is obtained from the top and bottom sections of the geometry and is the volume fraction in the top region divided by the sum of the volume fractions in the top and bottom as described in the main text for the experiment. Using this definition, if no solid is transported to the top, the parameter is equal to zero, and if the solid distribution is equal in the top and bottom the parameter is 1.

2 Additional mixing data

In addition to the data provided in the main text, here we provide space-rotation data for the higher concentration of particulates (ϕ_{ave} = 10.8%) in water Figure S 2 and in aqueous glycerol Figure S 3.

The evolution of particle distribution is assessed by generating a space-rotation plot from the x-ray image sequence. A line is taken from the midpoint of the image of the Couette gap at the top (red) and bottom (blue) as indicated in Figure S 2a. 10 images are averaged (10 x 10 ms exposure) and subsequent pixel lines are stacked. In the experiment the rotation rate was incremented in steps of 20rpm every 5 s. Hence the horizontal axis is calibrated to rotation. The resulting space (y-axis) –

rotation rate (x-axis) plot for the lower gap is shown in Figure S 2b and for the upper gap in Figure S 2c.

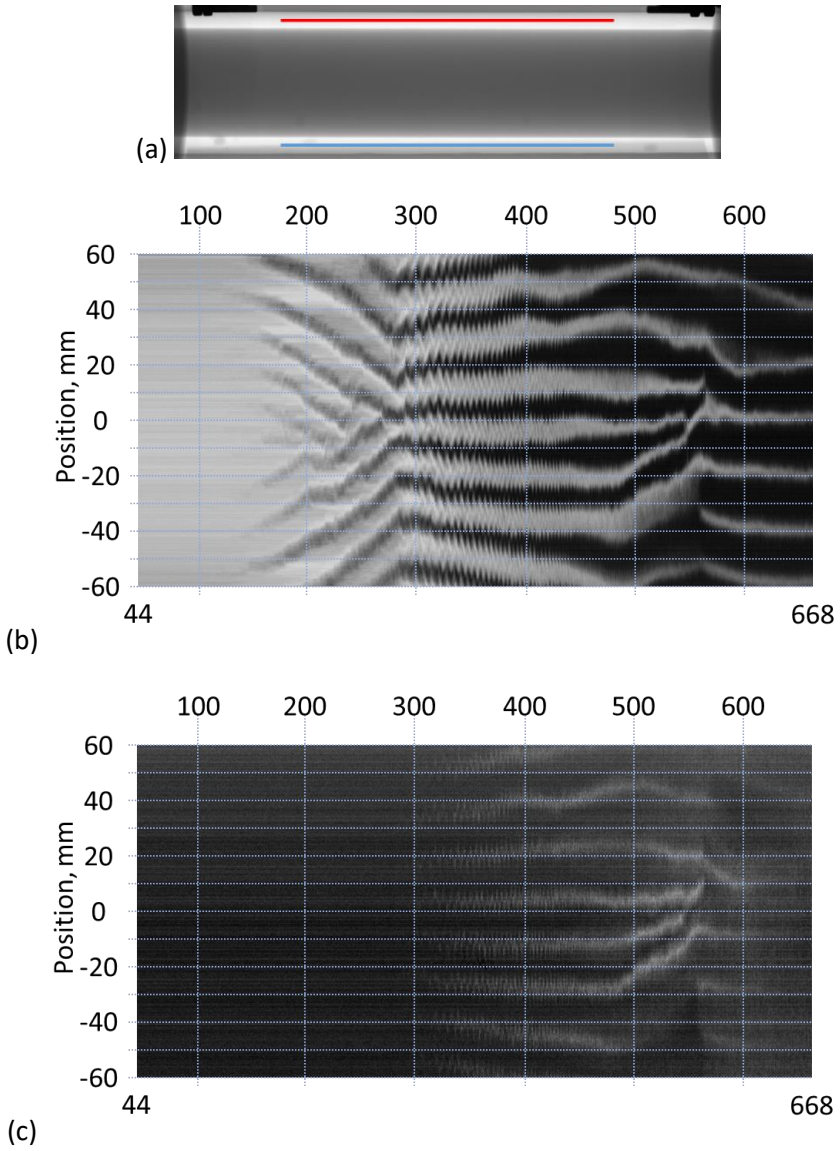

Figure S 2 (a) lines taken from the recorded image sequence in top (red) and bottom (blue) of the Couette for ϕ_{ave} = 10.8% particles in water, white indicates the presence of particles. (b) A space – rotation rate plot showing the distribution of particles at the bottom of the Couette (c) A space – rotation rate plot showing the distribution of particles at the top of the Couette. Numbers are rotation rate in rpm.

Focussing on Figure S 2b, as speed is increased several transitions are seen. At about 160 rpm (Ta=826) the bed is perturbed into regular mounds. As rotation is increased the mounds' position drifts, in this instance toward the centre of the Couette region. At about 280 rpm (Ta=1446) the mounds cease their drift but there is a periodic movement back and forth. The frequency of this periodic motion increases as the Couette rotation rate increases. Above about 470rpm (Ta=2427) we can no longer see the periodic oscillation (possibly because its frequency is too high for this measurement) but the mounds again are observed to drift. Finally above about 600rpm (Ta=3098) The residual mounds stop drifting but the period of the mounds is about 20mm (i.e. $\lambda/d \approx 4$). The foregoing description relates to the bed of particles at the bottom of the Couette. In Figure S 2c is shown the corresponding data for particles at the top of Couette. Here there are no particles observed until rotation has reached about 280 rpm, roughly commensurate with the onset of periodic bed movement in Figure S 2b. From

this rotation rate until about 460 rpm, the particle position appears to spatially oscillate as for the particle bed. Comparing Figure S 2b with Figure S 2c the particles at the top sit between the positions of the particles on the bottom. Above about 460 rpm, although particles can be seen in the lighter pixels, they appear to have become spatially more homogeneous, at least on a 100 ms time-scale, i.e. the averaging time in this data.

In Figure S 3 we show similar data to Figure S 2 but with a high concentration of particles in aqueous glycerol (21.3mPa.s) now as the background fluid. Although the rotation rate range (constrained by our instrumentation) is the same, of course the Taylor numbers are now 21.3x smaller. Surprisingly, in Figure S 3a we see the onset of bed movement occurs at about 160 rpm, very close to that seen in the water case above. Thus we speculate that this movement is not primarily driven by viscous forces, rather inertial forces, which are about the same in the two cases, dominate. Initially the bank positions are relatively stationary, however above about 300rpm, adjacent banks of particles interact with some growing at the expense of others. It should be noted that the rotation rate sweep in both Figure S 2 and Figure S 3 is conducted sufficiently quickly that the particles do not have time to reach a fully steady-state distribution. In contrast, in Figure 4b of the main text the images were acquired after 300s at each rotation speed and hence a steady state was achieved.

In both Figure S 3a and Figure S 3b pairs of lines develop, particularly above about 270 rpm. These are cross sections of ring structures that develop at both the top and the bottom of the Couette.

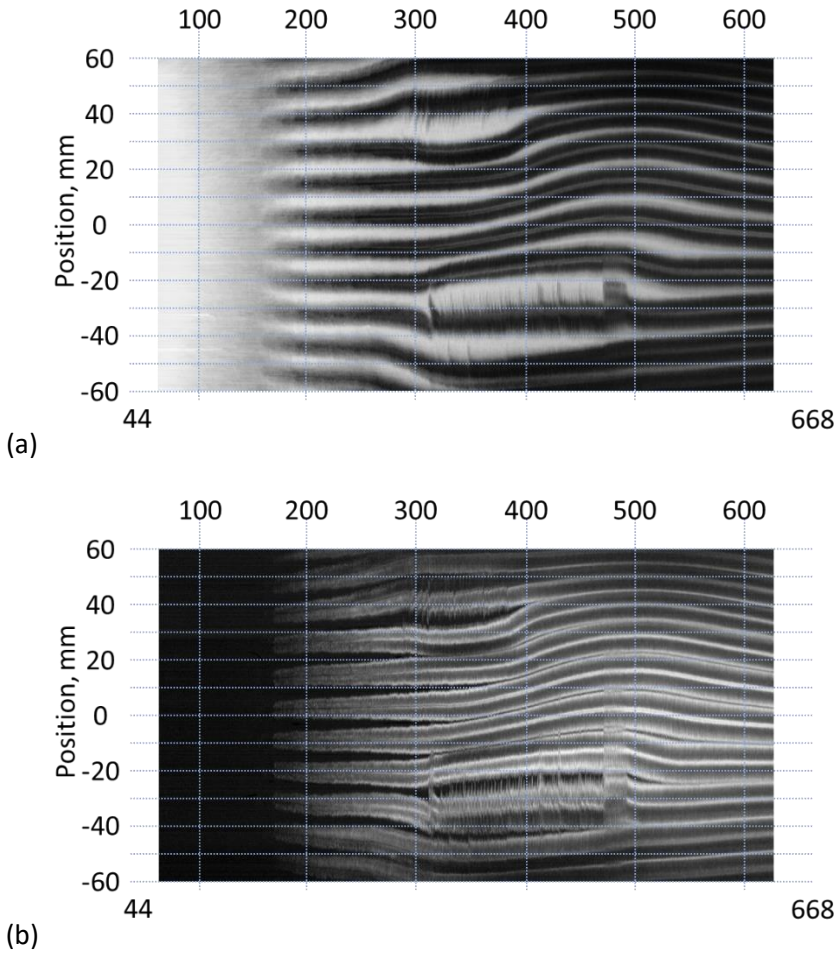

Figure S 3 (a) lines taken from the recorded image sequence in red (top) and blue (bottom) for for ϕ_{ave} = 10.8% particles in 21.3 mPa.s aqueous glycerol, white indicates the presence of particles. (b) A space –rotation rate plot showing the distribution of particles at the bottom of the Couette (c) A space –rotation rate plot showing the distribution of particles at the top of the Couette. Numbers are rotation rate in rpm.

3 Supplementary video

Also provided in the online version are experimental videos from which the still images provided in the main text are taken.

(i) Movie1. Particle distribution in aqueous glycerol as a function of rotation rate (inset) Figure 7 dataset. The background derived from the fluid only filled couette is subtracted, the image inverted so that particles appear white and the contrast/brightness adjusted for visual enhancement.

(ii) Movie2. Numerically generated video of wavey vortex evolution at 644rpm, Ta=202 and a particle volume concentration of 3.6%.